

## Interaction of Laser Beam and Gold Nanoparticles, Study of Scattering Intensity and the Effective Parameters

Mojtaba Servatkah<sup>\*1</sup>, Soheila Goodarzi<sup>1</sup>

<sup>1</sup> Department of Physics, Marvdasht Branch, Islamic Azad University, Marvdasht, Iran

(Received 20 Jun. 2017; Revised 23 Jul. 2017; Accepted 29 Aug. 2017; Published 15 Sep. 2017)

**Abstract:** In this paper, the optical properties of gold nanoparticles investigated. For this purpose the scattering intensity of a laser beam incident on gold nanoparticles has been studied using Mie theory and their respective curves versus different parameters such as scattering angle, wavelength of the laser beam and the size of gold nanoparticles are plotted. Investigating and comparison of the depicted plots show that the scattering intensity increases with increasing gold nanoparticles size up to 100 nm and further increasing of nanoparticles sizes leads to oscillating like behavior in the intensity patterns. Several peaks emerges in the patterns of intensity versus nanoparticle size. It was also found that for particles with sizes less than 100 nm the intensity patterns versus wavelength had a one peak about 520 nm while for the particles bigger than 100 nm there appears other maxima in different wavelength too. Changing the angle of scattering led to change in the intensity pattern of scattered light and its minimum value was detected at 90°. These results can be used in detecting cancerous tumors and in cancer therapy.

**Key words:** Gold nanoparticles, Laser radiation, Mie theory, Scattering intensity

### 1. INTRODUCTION

In recent years nanotechnology has become one of the most important and exciting forefront fields in Physics, Chemistry, Engineering and Biology [1]. Metal nanoparticles with different sizes and shapes, are the most considered nanostructures mostly because of their optical properties, which is dependent on the size and shape of nanoparticles. The surface plasmon resonance in metal nanoparticles undertakes their unique optical properties. This unique phenomenon to plasmonic (noble metal) nanoparticles leads to strong electromagnetic fields on the particle surface and consequently enhances all the

---

\* Corresponding author. E. mail: servatkah@miau.ac.ir

radiative properties such as absorption and scattering. This surface plasmon resonance differs the Plasmonic nanoparticles from other nano platforms such as semiconductors, quantum dots, magnetic and polymeric nanoparticles and leads to offering multiple properties useful for biological and medical applications [2]. The biomedical applications of metal nanoparticles started in the 1970s BY use of nano bio conjugates after the discovery of immune gold labeling by Faulk and Taylor [3].

Mie theory is used to study the interaction of light and spherical metal nanoparticles. In Mie theory the scattering intensity and cross section of light is calculated [4].

In this paper, based on Mie theory we have investigated the scattering intensity and the effective parameters of a laser beam incident on gold nano particles.

## **2. Gold nanoparticles, properties and applications**

The first metal colloid was discovered by Mikel Faraday in 1856. Faraday gold colloids had special electronic and chemical properties. Due to their optical and electronic properties Gold nano particles can be used for medical diagnosis and treatment of diseases and manufacturing sensors [5]. The stability and non-toxicity properties of gold nanoparticles along with their strong scattering and absorbing property, make them suitable in medical uses. The interaction between light and gold nanostructures is not only useful for the treatment of cancer but also for its diagnosis. Gold nanoparticles are very good at scattering and absorbing light. These gold nanoparticles have greater affinity for cancer cells than for noncancerous cells. This conjugated nanoparticle solution is added to healthy cells and cancerous cells. The concentration of gold nanoparticles in the cancerous cells is much more than the noncancerous cells so, if you see a well-defined cell glowing, that's cancer. Gold nanoparticles has been successfully used as a therapy for Rheumatoid arthritis and Cancer detection [5].

Weaknesses of common treatment methods in cancer therapy has faced it different challenges. Now, using nanoparticles as therapeutic agents provides a promising future for cancer treatment [6-14]. In the past few decades, photothermal therapy (PTT) has been studied widely to enhance cancer treatment efficiency [15–24]. Recently, the advantages of using hollow nanoparticles with respect to the applications in cancer therapy has been studied too [25].

Fig. 1 shows the concentration of gold nanoparticles in cancerous part of a mouse body which is used in diagnostic purpose.

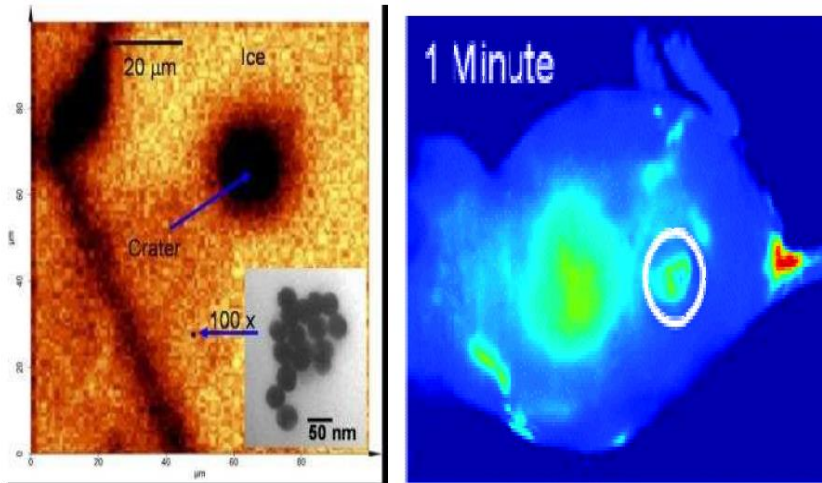


Fig. 1. Cancer Detection [5]

### 3. Mie theory

The general solution of Maxwell's equations for scattering from a sphere of arbitrary size was obtained in 1908 by Gustav Mie. The original Mie theory is restricted to plane wave scattering by a homogeneous sphere embedding in an isotropic and homogeneous medium [4].

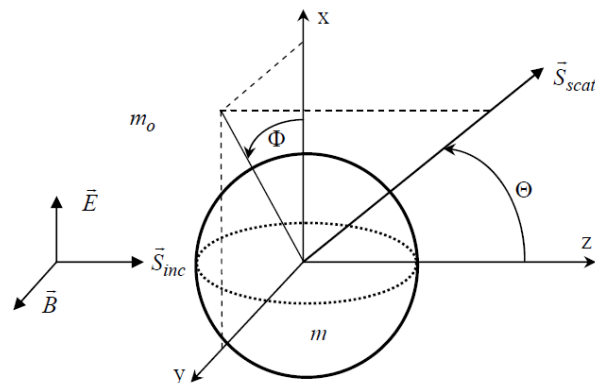


Fig. 2. Coordinate geometry for Mie scattering. [26]

Radiation intensity is the amount of energy that passes the unit area per unit time and is calculated using Mie theory [26].

$$I_{\varphi} = \frac{\lambda^2}{4\pi r^2} I_0 i_1(\theta) \sin^2(\varphi) \quad (1)$$

$$I_{\theta} = \frac{\lambda^2}{4\pi r^2} I_0 i_2(\theta) \cos^2(\varphi) \quad (2)$$

For each scattering angle  $(\theta, \varphi)$ , the Equations (1) and (2) represent the intensities of scattered radiation vertically and horizontally polarized with respect to the scattering plane, respectively, which is defined by the incident ray (of intensity  $I_0$ ) and the scattered ray, noting the polarization state of the incident ray as shown in Fig. 2.

If the equations are redefined in terms of the polarization states with respect to the scattering plane we have:

$$I_{VV} = \frac{\lambda^2}{4\pi r^2} I_0 i_1(\theta) \quad (3)$$

$$I_{HH} = \frac{\lambda^2}{4\pi r^2} I_0 i_2(\theta) \quad (4)$$

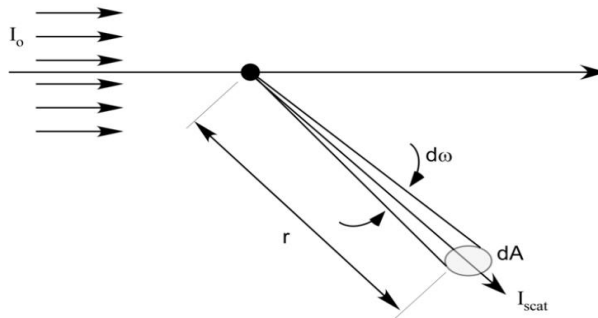


Fig. 3. Angular scattering intensity [8].

Here the subscripts refer to the state of polarization of the incident and scattered light, respectively, with orientation defined by the scattering plane. Specifically, the subscripts *VV* refer to both vertically polarized incident light and vertically polarized scattered light with respect to the scattering plane ( $\varphi = 90^\circ$ ). Similarly, the subscripts *HH* refer to both horizontally polarized incident light and horizontally polarized scattered light with respect to the scattering plane ( $\varphi = 90^\circ$ ).

If unpolarized incident light is considered, the scattering is given by the following formula:

$$I_{sca} = \frac{\lambda^2}{8\pi r^2} I_0 (i_1(\theta) + i_2(\theta)) \quad (5)$$

where,  $r$  is the distance to the object and  $I_0$  is the primary intensity.  $\lambda$  is the incident wavelength and  $i_1(\theta)$ ,  $i_2(\theta)$ , are the angular intensity functions calculated from the infinite series given by:

$$i_1(\theta) = \left| \sum_{n=1}^{\infty} \frac{2n+1}{n(n+1)} [a_n \pi_n(\theta) + b_n \tau_n(\theta)] \right|^2 \quad (6)$$

$$i_2(\theta) = \left| \sum_{n=1}^{\infty} \frac{2n+1}{n(n+1)} [a_n \tau_n(\theta) + b_n \pi_n(\theta)] \right|^2 \quad (7)$$

In these equations, the angular dependent functions  $\pi_n(\theta)$  and  $\tau_n(\theta)$  are expressed in terms of the Legendre polynomials by:

$$\pi_{mn}(\theta) = \frac{m P_{mn}(\cos \theta)}{\sin \theta} \quad (8)$$

$$\tau_{mn}(\theta) = \frac{d P_{mn}(\cos \theta)}{d \theta} \quad (9)$$

$a_n$  and  $b_n$  are Mie coefficients defined as:

$$a_n = \frac{\psi_n(\alpha) \psi_n(m\alpha) - m \psi_n(m\alpha) \psi_n(\alpha)}{\xi_n(\alpha) \psi_n(m\alpha) - m \psi_n(m\alpha) \xi_n(\alpha)} \quad (10)$$

$$b_n = \frac{m \psi_n(\alpha) \psi_n(m\alpha) - \psi_n(m\alpha) \psi_n(\alpha)}{m \xi_n(\alpha) \psi_n(m\alpha) - \psi_n(m\alpha) \xi_n(\alpha)} \quad (11)$$

where  $\alpha$  is dimensionless size parameter given by the expression

$$\alpha = \frac{2\pi a}{\lambda} \quad (12)$$

where  $a$  is the spherical particle radius and  $m$  is the refractive index of the scattering particle, and is commonly represented by the complex notation defined as

$$m = n - ik \quad (13)$$

Where,  $n$  indicates the refraction index of light and  $k$  indicates the absorption coefficient.  $\psi_n(\alpha)$  and  $\xi_n(\alpha)$  are Riccati – Bessel and Riccati – Hankel functions expressed as:

$$\psi_n(\alpha) = \sqrt{\frac{\pi\alpha}{2}} J_{n+1/2}(\alpha) \quad (14)$$

$$\xi_n(\alpha) = \sqrt{\frac{\pi\alpha}{2}} H_{n+1/2}(\alpha) \quad (15)$$

These equations show that the scattering angle, nanoparticle size and wavelength of the incident beam are the effective factors on the scattering intensity.

In this paper, we simulate the interaction of a Laser Beam with gold nanoparticles. In these simulations some parameters such as optical constants of gold nanoparticles versus the wavelength of laser are obtained from the table of ref.

[9]. Curves of the scattering intensity versus parameters such as scattering angle, wavelength of the laser and size of nanoparticles are simulated.

#### **4-1. The effect of nanoparticle size on the scattering intensity**

To simulate the effect of nanoparticle size on the scattering intensity, the curves of the scattering intensity versus the size of nanoparticles are plotted using Eq.'s 3-5.

In the plotted curves of scattering intensity  $R=2a$  is the particle diameter which is assumed from 5 nm to 100 nm. The refractive index of gold nanoparticle,  $m$  at different wavelength's is different so in our calculations their respective values are taken from [27,28]. The primary intensity of incident beam is taken as  $5 \mu w m^{-2}$ . The distance to the object is assumed to be 5 cm and scattering angle is considered  $45^\circ$ .

In Fig. 4 the intensities  $I_{VV}$ ,  $I_{HH}$  and  $I_{SCA}$  are plotted versus particle diameter in three wavelengths 413 nm, 532 nm and 617 nm. These plots show that the scattering intensity increase with increasing gold nanoparticle size from 0 to 100 nm. Beyond 100 nm the intensity curves change their behavior. They have oscillating like behavior. It can be seen from Fig. (4-a) that  $I_{SCA}$  reaches its maximum for nano particles with diameters about 180 nm, 420 nm and 600 nm for the incident wavelength of 413 nm. These values for  $I_{VV}$  and  $I_{HH}$  are a little different. By increasing the diameters from 700 nm to 900 nm the scattered intensity increases more rapidly. Fig. (4-b) and (4-c) the intensities  $I_{VV}$ ,  $I_{HH}$  and  $I_{SCA}$  are plotted versus particle diameter. As it can be seen from these figures the scattering intensity patterns change be changing the wavelength of incident laser beam. For 532 nm wavelength the values of the peaks of intensity pattern are greater than the peak's values at 413 nm and 617 nm. Moreover the maxima have approximately the same value.

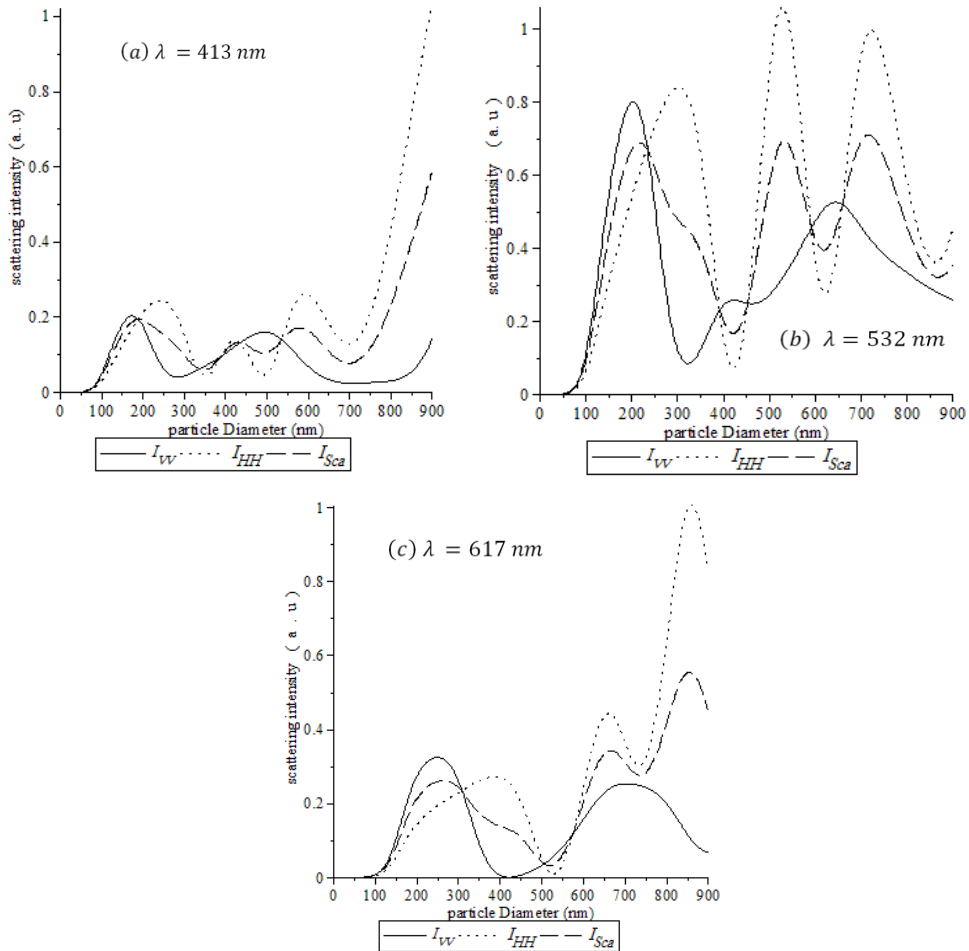


Fig. 4 Scattering intensities  $I_{VV}$ (—),  $I_{HH}$ (...),  $I_{Sca}$ (--) versus size of gold nanoparticle for different wavelength a) 413 nm b) 532 nm c) 617 nm

Fig. 5 shows the intensity curves  $I_{VV}$ ,  $I_{HH}$  and  $I_{Sca}$  versus particle diameters for three wavelengths 413, 532 and 617 nm. From Fig. (5-a,b,c) it can be observed that the scattering intensity increases with increasing the incident wavelength. It is also seen from these curves that the peak of intensity patterns tends to shift towards the particles with larger diameters for instance in fig. (5-a) the first peak is observed at 180, 200 and 300 nm particle diameter for 413 nm, 532 nm and 617 nm incident wavelength, respectively.

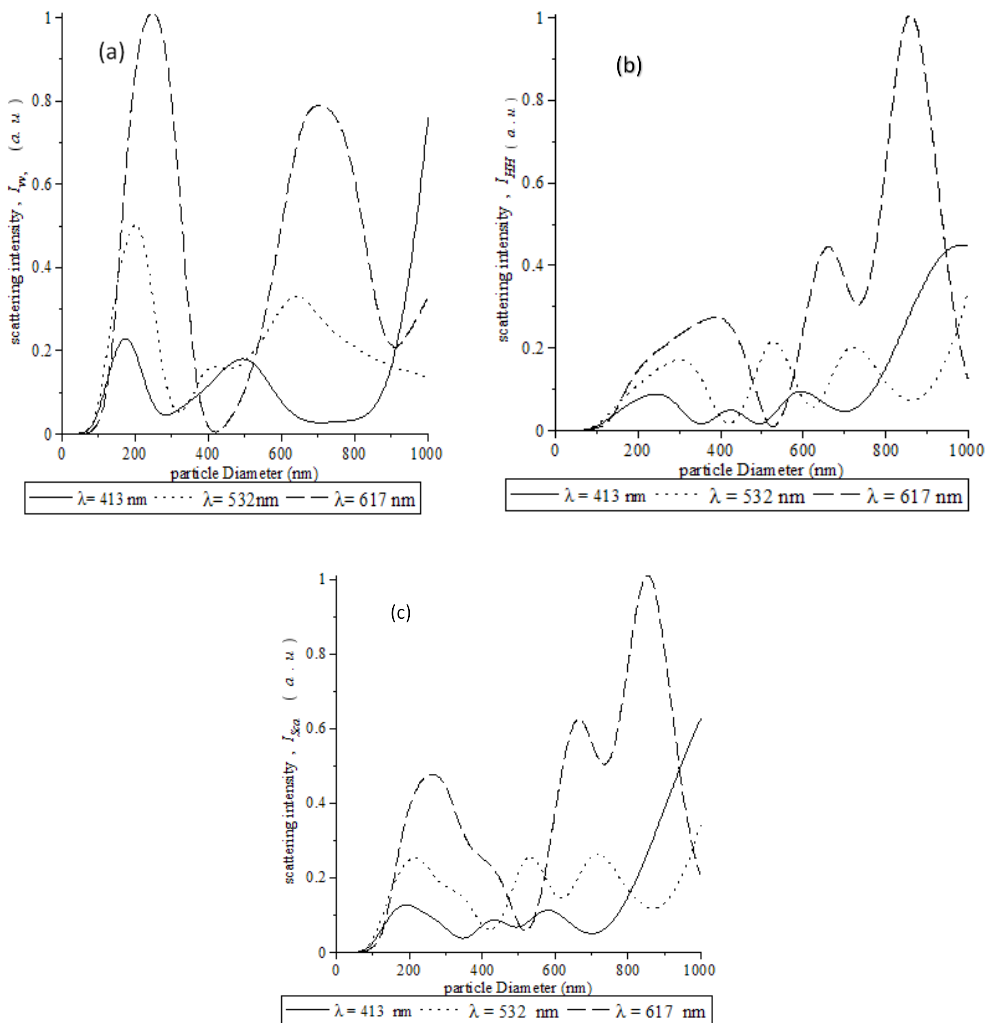


Fig. 5- a)  $I_{vv}$ , b)  $I_{HH}$  and c)  $I_{sca}$  versus size of gold nanoparticle for different wavelength 413 nm(—), 532 nm(...) and 617 nm(---)



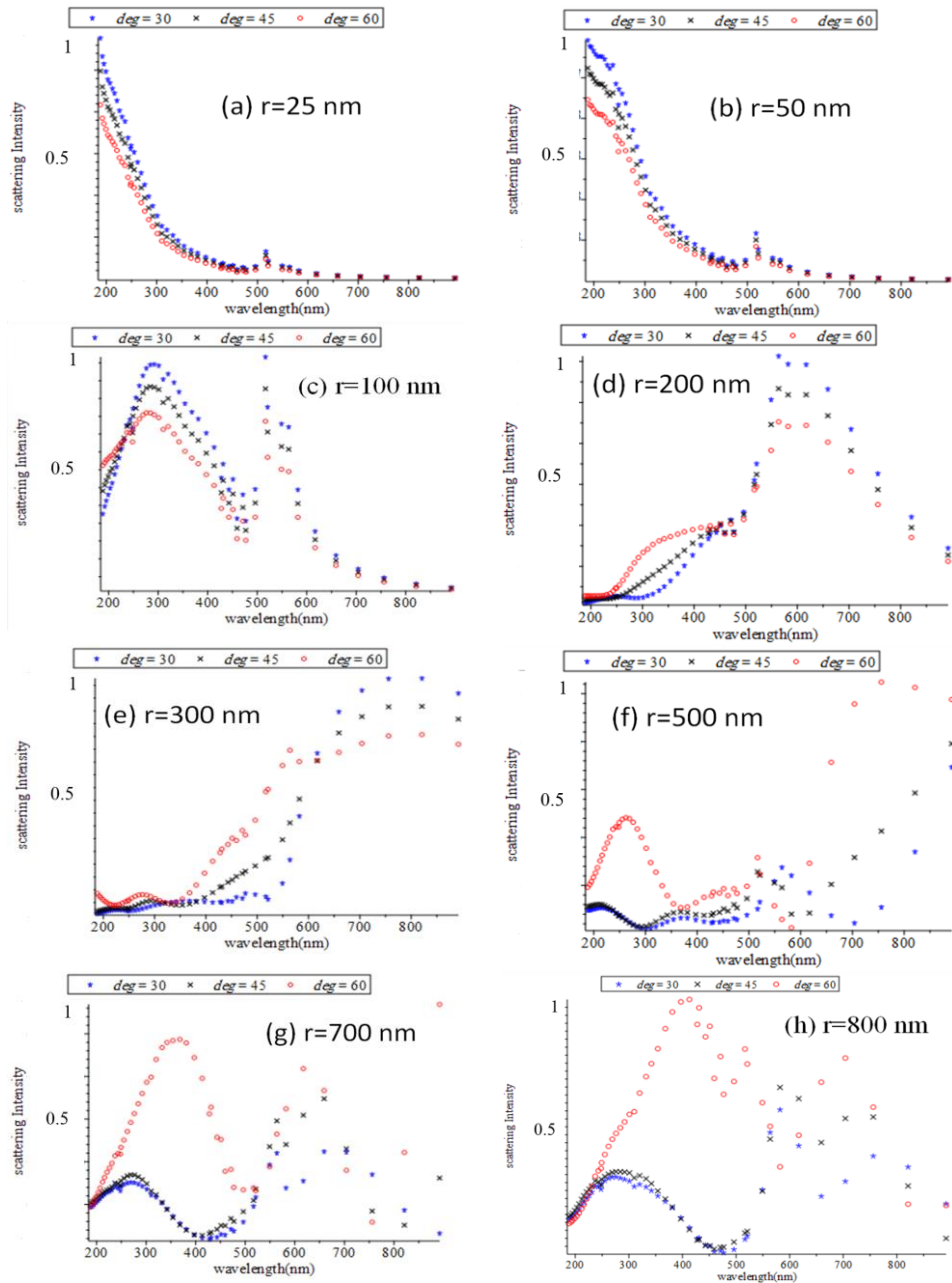


Fig. 6. Curves of the scattering intensity versus wavelength of the incident laser beam for different scattering angles,  $\theta=30^\circ$  (blue),  $45^\circ$  (black),  $60^\circ$  (red) and different nanoparticle radius.

#### **4-2. The effect of wavelength of the incident beam on the scattering intensity**

The curves of the scattering intensity versus wavelength of the incident laser beam are plotted in Fig. 6. The distance to the object is taken 5 cm and the scattering angle assumed to be 30°, 45° and 60° in each plot. The curves are plotted for different nanoparticle radii.

Fig. (6-a) shows that the scattering intensity decreases with increasing wavelength of the incident laser beam for the nanoparticle radius of 25 nm. As the wavelength further increases the peak of scattering intensity emerges at about  $\lambda=520$  nm (at the middle of visible spectrum). By increasing the nanoparticle radius to 50 nm the peak of scattering intensity get bigger value (fig. (6-b)). In fig. (6-c) to (6-h) it is observed that by increasing  $r$ , new peaks of scattering intensity in different wavelength emerges. It can be seen from these plots that the behavior of scattering intensity in different scattering angles more or less are the same up to  $r=300$  nm. As  $r$  increases to 500 nm the behavior of the scattering intensity pattern at the scattering angle 60° (red dotted curve) changes. It is also seen that the peak of scattering intensity at 60° emerges at different wavelength and they have bigger values.

#### **4-3. The effect of scattering angle on the scattering intensity**

The simulated curves of the scattering intensity versus scattering angle are plotted in Fig. 7. In these plots the sizes of gold nanoparticles are assumed to be 20 nm, 50nm and 100 nm. From fig. (7-a) it can be seen that the intensity curves  $I_{VV}$ ,  $I_{HH}$  and  $I_{SCA}$  behave the same for different nanoparticles sizes when the wavelength of the incident laser beam is 413 nm. It is also seen that the intensity pattern of  $I_{VV}$  does not change by changing the scattering angle while the other two intensities  $I_{HH}$  and  $I_{SCA}$  change from value of 1 to a minimum of 0 and 0.5 at  $\theta=\pi/2$ , respectively. Fig. (7-b) and (7-c) show the same plots for  $\lambda= 532$  nm and  $\lambda= 617$  nm respectively. As it is seen in these figures the patterns of intensities began to have approximately different behavior. The value of the intensities in these fig.'s are more distinct from 0.9 for  $R=100$  nm to 1 for  $R= 20$  nm particle size. The difference of intensities values at  $\theta=0$  becomes more distinct by increasing  $\lambda$  to 617 nm (Fig. (7-c)).

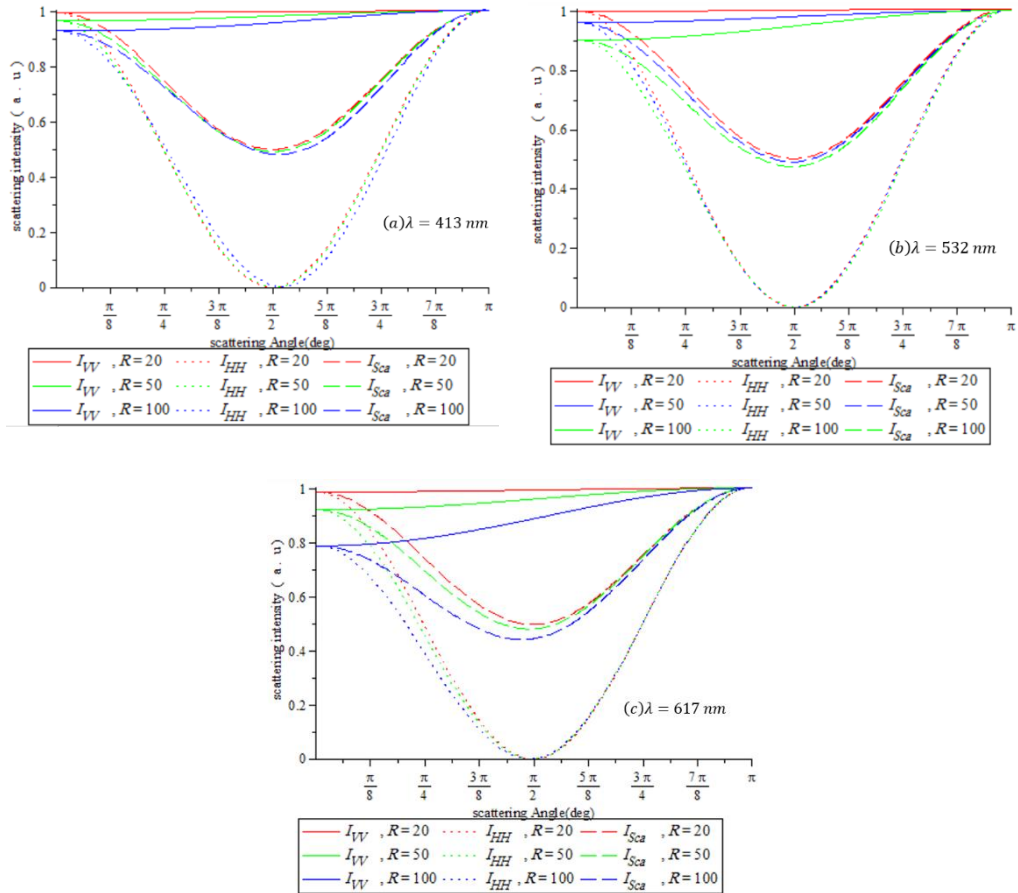


Fig. 7. Plots of scattering intensities  $I_{VV}$  (—),  $I_{HH}$  (...) and  $I_{ScA}$  (--) versus scattering angle for incident wavelengths of a) 413 nm, b) 532 nm, c) 617 nm and different nanoparticle sizes 20 nm (red), 50 nm (green) and 100 nm (blue).

## 5. Conclusion

The interaction of Laser Beam and gold nanoparticles has been investigated in this work. Scattering intensity and the effective parameters on the scattering intensity are calculated using Mie theory. Curves of the scattering intensity versus different parameters such as scattering angle, wavelength of the incident laser beam and nanoparticles size are simulated. Simulations and calculated results show that the scattering angle, refractive index, absorption coefficient of the nanoparticle, nanoparticle size and wavelength of the incident beam are the effective factors on the scattering intensity of light from gold nanoparticles.

The results also show that the scattering intensity increase with increasing gold nanoparticle size to 100 nm and by further increasing nanoparticle size the pattern shows an oscillating behavior. It was observed that by increasing the wavelength of the laser beam the scattering intensities increase too. Another important parameter on the scattering intensities is the wavelength and size of the nanoparticles. It was seen from the figures that the intensity patterns of gold nanoparticle has a peak around 520 nm wavelength and the value of this peak becomes bigger by increasing the size of nanoparticles, but further increase in the size leads to emerging other peaks in the intensity pattern of scattering light at other wavelength. Besides, It was found that the intensity pattern of scattering light versus scattering angle have the same behavior for different nanoparticle sizes and the values of the intensities become more distinct by increasing the incident laser beam wavelength.

## REFERENCES

- [1] Charles P. Poole, Jr. Frank J. Owens, *Introduction to nanotechnology*, Wiley-Interscience, 2003.
- [2] X. Huang and M.A. El-Sayed, *Gold nanoparticles: optical properties and implementation in cancer diagnosis and photothermal therapy*, Journal of advanced research, 1 ( 2010) 13-28.
- [3] Matthews., Kanwar, R.K., Zhou, Sh., Punj, V., Kanwar, J.R., *Applications of Nanomedicine in Antibacterial Medical Therapeutics and Diagnostic*, The Open Tropical Medicine Journal, 3 (2010) 1-9.
- [4] G. A. Mie, *contribution to the optics of turbid media, especially Colloidal metallic suspensions*, Ann. Phys., 25 (1980) 377-445.
- [5] P.M. Prajapati, Y. Shah and D.J. Sen, *Gold Nanoparticles: A new approach for cancer Detection*, Journal of Chemical and Pharmaceutical Research, 2 (1) (2010) 30-37.
- [6] L. Brannon-Peppas and Blanchette, *Nanoparticle and targeted systems for cancer therapy*, Advanced Drug Delivery Reviews, 56 (2004) 1649-1659.
- [7] J. Yu, D. Y. Huang, M. Z. Yousaf, Y. L. Hou and S. Gao, *Magnetic nanoparticle-based cancer therapy*, Chin Phys B. 22 (2013) 027506.
- [8] P. F. Jiao, H. Y. Zhou, L. X. Chen and B. Yan, *Cancer-Targeting Multifunctionalized Gold Nanoparticles in Imaging and Therapy*, Curr. Med. Chem. 18 (14) (2011) 2086-2102.
- [9] S . Jain, D. G. Hirst and J. M. O'Sullivan, *Gold nanoparticles as novel agents for cancer therapy*, Br. J. Radiol., 85 (2012) 101.

- [10] M. Wang and M. Thanou, *Targeting nanoparticles to cancer*, Pharmacol. Res. 62 (2010) 90.
- [11] A. Kumar, H. Ma, X. Zhang, K. Huang, S. Jin, J. Liu, T. Wei, W. Cao, G. Zou and X. J. Liang, *Gold nanoparticles functionalized with therapeutic and targeted peptides for cancer treatment*, Biomaterials, 33 (2012) 1180-1189.
- [12] E. C. Dreaden, L.A. Austin, M.A. Mackey and M. A. El-Sayed, *Size matters: gold nanoparticles in targeted cancer drug delivery*, Therapeutic Delivery, 3 (4) (2012) 457.
- [13] P. R. Gil and W. J. Parak, *Composite Nanoparticles Take Aim at Cancer*, ACS Nano, 2 (2008) 2200-2205.
- [14] X. Huang and M. A. El-Sayed, *The Ongoing History of Thermal Therapy for Cancer*, Alexandria J. Med. 47 (2011) 1.
- [15] E.S. Glazer and S. A. Curley, *The Ongoing History of Thermal Therapy for Cancer*, Surg. Oncol. Clin. N. Am. 20 (2011) 229.
- [16] X. L. Yue, F. Ma and Z. F. Dai, *Multifunctional magnetic nanoparticles for magnetic resonance image-guided photothermal therapy for cancer*, Chin. Phys. B, 23 (2014) 044301.
- [17] E.S. Shibu, M. Hamada, N. Murase and V. Biju, *Nanomaterials formulations for photothermal and photodynamic therapy of cancer*, J. Photochem. Photobiol. C Photochem. Rev. 15 (2013) 53.
- [18] E. B. Dickerson, E.C. Dreaden, X. Huang, I. H. El-Sayed, H. Chu, S. Pushpanketh, J.F. McDonald and M. A. El-Sayed, *Gold nanorod assisted near-infrared plasmonic photothermal therapy (PPTT) of squamous cell carcinoma in mice*, Cancer Lett. 269 (2008) 57-66.
- [19] A. M. Gobin, M. H. Lee, Halas, N.J. James, R.A. Drezek and J.L. West, *Near-Infrared Resonant Nanoshells for Combined Optical Imaging and Photothermal Cancer Therapy*, Nano Lett. 7 (2007) 1929.
- [20] M.P. Melancon, M. Zhou and C.Li, *Cancer Theranostics with Near-Infrared Light-Activatable Multimodal Nanoparticles*, Acc. Chem. Res. 44 (2011) 947.
- [21] W. Il. Choi, A. Sahu, Y. H. Kim and G. Tae, *Photothermal Cancer Therapy and Imaging Based on Gold Nanorods*, Ann. Biomed. Eng. 40 (2012) 534.
- [22] N. Rozanova and J. Zhang, *Photothermal ablation therapy for cancer based on metal nanostructures*, Sci. China, Ser. B Chem. 52 (2009) 1559.

- [23] M.A. MacKey, M. R. K. Ali, L.A. Austin, R. D. Near and M.A. El-Sayed, *The Most Effective Gold Nanorod Size for Plasmonic Photothermal Therapy: Theory and In Vitro Experiments*, J. Phys. Chem. B, 118 (2014) 1319.
- [24] D.K. Kirui, S. Krishnan, A.D. Strickland and C.A. Batt, *PAA-Derived Gold Nanorods for Cellular Targeting and Photothermal Therapy*, Macromol. Biosci. 11 (2011) 779.
- [25] S. Abbasi, M. Servatkhah, M.M. Keshtkar, *Advantages of using gold hollow nanoshells in cancer photothermal therapy*, Chinese Physics B, 25 (2016) 087301.
- [26] M. Quinten, *Optical Properties of Nanoparticle Systems*, Wiley-VCH Verlag & Co . KGaA, Boschstr. Weinheim, Germany, 2011.
- [27] H.C. van de Hulst, *Light scattering by small particles*. John Wiley & Sons, New York, 1957.
- [28] P. B. Johnson and R.W. Christy, *Optical Constants of the Noble Metals*, PHYSICAL REVIEW B, 6 (12) (1972) 4370- 4378.